Electron Vortices Produced by Ultraintense Laser Pulses

S. V. Bulanov and M. Lontano
Institute for Plasma Physics, CNR, Milan, Italy

T. Zh. Esirkepov
Moscow Institute for Physics and Technology, Dolgoprudnyi, Russia

F. Pegoraro
Department of Theoretical Physics, University of Turin, Turin, Italy

A. M. Pukhov
Max-Planck-Institute for Quantum Optics, Garching, Germany
(Received 21 November 1995)

Particle-in-cell simulations show that finite width and length laser pulses subject to relativistic self-focusing propagate in an underdense plasma in a "bullet" shape and produce a quasistatic magnetic field. This field remains behind the pulse and forms a magnetic wake associated with a row of electron fluid vortices which are described by the Hasegawa-Mima equation. The vortices propagate much more slowly than the pulse and evolve into an antisymmetric configuration which is shown to be stable when the distance between its vortices is greater than the electron skin depth. [S0031-9007(96)00103-2]

PACS numbers: 52.40.Nk, 52.35.Ra, 52.65.Rr

Vortex dynamics is considered to be important in explaining a wide variety of nonlinear processes in magnetized plasmas and to represent the final stage of the development of turbulence [1–3]. In this Letter we discuss a new area of application of vortex physics and show that electron fluid vortices are produced in the interaction of an ultrashort high-intensity laser pulse with an initially unmagnetized plasma. A laser pulse with finite length and width, and with sufficiently high intensity, is subject to relativistic self-focusing and can propagate in the shape of a short, narrow "bullet" [4]. As was shown by computer simulations [5,6], a quasistatic magnetic field is produced in the vicinity of the region where the electromagnetic radiation is localized. We address here the question of what geometrical structure this quasistatic magnetic field can be expected to develop behind the laser pulse.

First we present the results of a particle-in-cell (PIC) computer simulation of the interaction of a laser pulse in an underdense plasma, which we performed in order to analyze the shape and the time development of the quasistatic magnetic field. We used the 2X3V-PIC relativistic electromagnetic code described in [4]. All physical variables depend on two spatial coordinates x and y. Ions are treated as a fixed charge neutralizing background. A 512×256 grid is used with approximately 10^6 particles, the plasma begins at $x = 5\lambda$ and is preceded by a vacuum region and the pulse is initialized at $t = -10\pi/\omega$ outside the plasma at the $x = 0$ boundary. The laser pulse is linearly polarized with its electric field directed along the z direction, so that the z component of the magnetic field is initially zero. In Fig. 1 we present the results obtained in the case of an underdense plasma ($\omega_{pe}/\omega = 0.45$) of a pulse with frequency ω, dimensionless amplitude $a \equiv eE/m_e\omega c = 3$ ($a > 1$ for relativistic pulses), and initial width and length $\lambda_\perp = 5\lambda$ and $\lambda_\parallel = 12\lambda$, respectively. For these parameters the pulse power $P = a^2\lambda_\perp$ is greater than the threshold for relativistic self-focusing. As a result, the pulse is focused and propagates in the shape of a narrow, finite length bullet as shown in Fig. 1. A vortex row is formed behind the pulse: Solid (dotted) lines correspond to constant positive (negative) values of the z component of the magnetic field. Since $\nabla \times \mathbf{B}$ is proportional to the electron fluid velocity $\mathbf{v}$, these isomagnetic curves also correspond to the stream lines of the electron motion. The structure and magnitude of the magnetic field correspond to that of a narrow central current sheet directed along x and carried by relativistic electrons produced by the wave break of the plasma

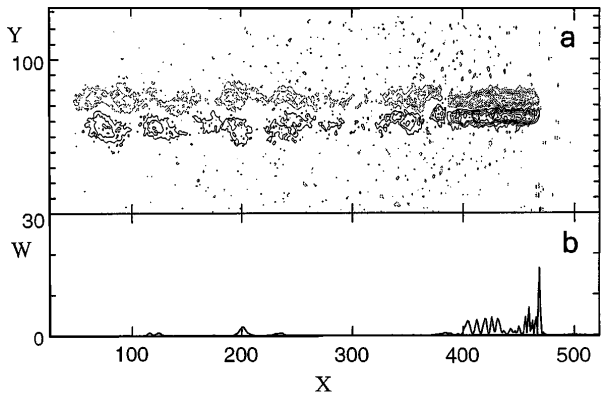

FIG. 1. Magnetic wakefield generated by an ultrashort laser pulse in an underdense plasma: (a) distribution of the quasistatic magnetic field; (b) e.m. energy density on the pulse axis ($X \equiv kx = 2\pi x/\lambda, Y \equiv ky = 2\pi y/\lambda$, B is normalized on $m_e\omega c/e$).

 0031-9007/96/76(19)/3562(4)$10.00

wakefield [6]. Plasma charge neutrality is ensured by two return current sheets which run at the periphery due to opposite current repulsion. This repulsion is the basis for the magnetic field formation through the development of the Weibel instability. The occurrence of wave breaking makes these laser plasma regimes less interesting from the point of view of laser wakefield acceleration, even if *per se* the focusing properties of the magnetic field would be beneficial, as discussed in Refs. [7,8]. Following Ref. [6], we estimate the magnetic field strength as $B = a(m_e\omega c/e)(\omega_{pe}/\omega)^2$. We see that the current sheet develops an instability which tends to bend it and to produce a vortex row: The small scale vortices merge and an asymmetry appears in the vortex row. The size of these vortices is typically of the order of or larger than the collisionless skin depth c/ω_{pe} and the period of their motion is much longer than that of the Langmuir waves. The propagation velocity of the vortex row along x is $\approx \frac{1}{40} v_g$, much smaller than the group velocity $v_g \approx c$ of the laser pulse. We also see the development of a small scale instability that generates a short wavelength turbulence of "vortex pairs" at a distance $\approx 2\pi c/\omega_{pe}$ behind the head of the laser pulse [Fig. 1(a)]. In the distribution of the electromagnetic energy density shown in Fig. 1(b), we see that the pulse is localized in a well-delimited region and that its leading part becomes sharper.

In the remaining part of this Letter we will investigate the bending instability of a finite width current sheet that has been observed in the PIC simulations. We invoke the freezing of the z component of the rotation of the generalized momentum $\nabla \times [\mathbf{p} - (e/c)\mathbf{A}]$ into the electron fluid. Here $\mathbf{p}$ is the electron momentum and $\mathbf{A}$ is the vector potential. Since their motion is slow compared to the Langmuir time and their velocity is much smaller than speed of light c, the electron fluid can be regarded as incompressible. This leads to the following relationship between the electron velocity and the magnetic field: $\mathbf{v} = -(c/4\pi en)\nabla \times \mathbf{B}$, so that, taking $\mathbf{B}$ to be along the z axis, we obtain

$$(\partial/\partial t + \hat{z} \times \nabla B \cdot \nabla)(\Delta B - B) = 0, \qquad (1)$$

where the time and space units are $\omega_{Be}^{-1} = a^{-1}(\omega/\omega_{pe}^2)$, and c/ω_{pe}, respectively. Equation (1) is known as the Charney equation or the Hasegawa-Mima (HM) equation in the limit of zero drift velocity or the electron-magnetohydrodynamics equation [1,2,9,10]. As is well known (see Refs. [3,11]) Eq. (1) has a discrete vortex solution for which the generalized vorticity is localized at the points $\mathbf{r} = \mathbf{r}_j$: $\Omega = \Delta B - B = \sum_j \Gamma_j \delta(\mathbf{r} - \mathbf{r_j}(t))$. Here Γ_j are constants and $\mathbf{r} = (x, y)$. Then we have $B = \sum_j B_j$, $\quad B_j(\mathbf{r}, \mathbf{r}_j(t)) = -(\Gamma_j/2\pi)K_0(|\mathbf{r} - \mathbf{r_j}(t)|)$. Here and below $K_n(\xi)$ are modified Bessel functions. The curves $\mathbf{r_j}(t)$ are determined by the characteristics of Eq. (1) $\dot{\mathbf{r}}_j = \hat{z} \times \nabla \cdot \sum_{k \neq j} B_k(\mathbf{r}_j(t), \mathbf{r}_k(t))$. From these expressions the equation of motion of the vortices,

$$\dot{x}_j = -\frac{1}{2\pi} \sum_{k \neq j} \Gamma_k \frac{y_j - y_k}{r_{jk}} K_1(r_{jk}),$$
$$\dot{y}_j = \frac{1}{2\pi} \sum_{k \neq j} \Gamma_k \frac{x_j - x_k}{r_{jk}} K_1(r_{jk}), \qquad (2)$$

follows, where $r_{jk} = |\mathbf{r_j} - \mathbf{r_k}| = [(x_j - x_k)^2 + (y_j - y_k)^2]^{1/2}$. We will assume that all vortices have the same absolute amplitude and take $|\Gamma_j| = 1$.

We consider the problem of the stability of an infinite vortex chain. In the initial equilibrium the vortices have coordinates $x_j^0 = js$, $y_j^0 = 0$, $-\infty < j < +\infty$ and amplitudes $\Gamma_j = 1$. If the distance s between neighboring vortices is much smaller than 1 (in dimensional units much smaller than the collisionless skin depth), for $s \ll |y| \ll 1$ the chain separates two subregions, an upper and lower one, with opposite electron velocity along x, $v_x = \mp U = \mp 1/(2s)$. This is equivalent to a vortex film with uniform surface density of generalized vorticity $-1/s$. Far from the film for $|y| \gg 1$, both B and v_x tend to zero exponentially. This structure corresponds to two, oppositely directed, electric current sheets that have a width of order one. In the analysis of a vortex chain stability we extend the approach developed in hydrodynamics [12] to the Hasegawa-Mima point vortices. We consider the motion of the jth vortex with coordinates $x = js + x_j(t)$ and $y = y_j(t)$. Because of the translational invariance of the initial configuration we seek solutions of Eqs. (2), linearized around the equilibrium configuration, of the form $x_j = X \exp[\gamma t + i(j\varphi)]$, $y_j = Y \exp[\gamma t + i(j\varphi)]$, with $0 < \varphi < 2\pi$. If φ is small, the perturbation has the form of a sinusoidal wave with wavelength $\lambda = 2\pi/\kappa = 2\pi s/\varphi$, where κ is the wave number. The perturbations grow exponentially in time, and the growth rate γ is given by

$$\gamma = \frac{1}{\pi}\left\{\left[\sum_{j=1}^{\infty} \frac{K_1(js)}{js}(1 - \cos j\varphi)\right] \times \left[\sum_{k=1}^{\infty}\left(K_2(ks) - \frac{K_1(ks)}{ks}\right)(1 - \cos k\varphi)\right]\right\}^{1/2}. \qquad (3)$$

If $s \ll 1$ and $\varphi \gg 2\pi s$, $\lambda < 1$ and Eq. (3) reproduces the result obtained in Ref. [12]: $\gamma = \varphi(2\pi - \varphi)/4\pi s^2$. When $\varphi \ll 1$, we have $\gamma \approx \varphi/2s^2 = \kappa U$, where $U = 1/(2s)$, which coincides with the growth rate of the Kelvin-Helmholtz instability. For $s \ll 1$ and $\varphi < 2\pi s$, i.e., for wavelengths greater than the width of the current sheet ($\lambda > 1$), Eq. (3) gives $\gamma = \varphi^2/\pi s^3 = \kappa^2 U/2\pi$. In the long wavelength limit the instability becomes slow compared to the Kelvin-Helmholtz instability. In the limit $s \gg 1$, when the distance between two neighboring vortices is larger than one, Eq. (3) gives $\gamma \approx (1 - \cos\varphi)\exp(-s)/s\sqrt{2\pi}$ and the instability is exponentially slow.

In order to determine the nonlinear stage of the vortex film instability, we have performed a numerical integration of Eq. (1). At the initial time the generalized vorticity

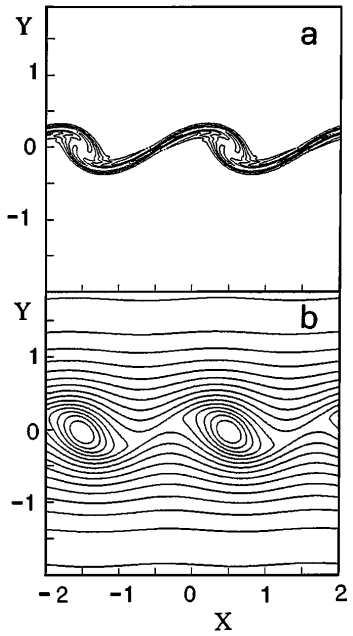

FIG. 2. Bending instability of a vortex film. (a) Curves of equal generalized vorticity Ω for $t = 19\omega_{Be}^{-1}$, lengths are normalized to c/ω_{pe}, the initial vorticity is $\Omega = 1$: $\Omega_{\min} = -0.03, \Omega_{\max} = 1.3$; (b) isomagnetic curves: $B_{\min} = -0.037, B_{\max} = 0.1$.

is assumed to be localized in a region narrow in the y direction and infinitely long in the x direction. Then a small amplitude perturbation that depends on both x and y is superimposed. The width of the vortex layer is $0.05c/\omega_{pe}$, while the perturbation wavelength is equal to $2c/\omega_{pe}$. This corresponds to the case when the width of the vortex layer is much shorter than the collisionless skin depth while the perturbation wavelength is longer. In Fig. 2(a) we see the bending of the chain and the formation of bunches of generalized vorticity on the vortex film. The isomagnetic curves have the form of "squint cat eyes," as shown in Fig. 2(b). This instability slows down with time. This can be explained by the exponential decreasing of the instability growth rate when the distance between neighboring vortices becomes of order or larger than 1, consistent with the analytical results obtained above.

Now we consider the stability of a thin current sheet. We note that the instability of a current sheet against bending in the framework of the MHD description has been investigated in Ref. [13]. Let us consider a double chain of opposite vortices in which the coordinates and the amplitudes of point vortices are equal to $x_j^0 = js + Ut$, $y_j^0 = \frac{1}{2}q$, $-\infty < j < +\infty$, $\Gamma_j = -1$ for the upper chain, and $x_k^0 = (k + \sigma)s + Ut$, $y_k^0 = -\frac{1}{2}q$, $-\infty < k < +\infty$, $\Gamma_k = 1$ for the lower chain, respectively. The distance between neighboring vortices in a chain is s, the distance between the chains in the y direction is q, and the lower chain is shifted along the x direction by σs: $\sigma = 0$ and $\sigma = 1/2$ correspond to the symmetrical and to the antisymmetrical configurations, respectively. Here

$$U = \frac{q}{\pi}\sum_{k=0}^{\infty}\frac{K_1(\rho_k')}{\rho_k'}, \quad \rho_k' = [(k + \sigma)^2 s^2 + q^2]^{1/2} \tag{4}$$

is the global velocity of the double chain in the x direction. When $s \ll 1$ and $q \ll 1$ we recover known results [12]: $U = (1/2s)\coth(\pi q/s)$ for $\sigma = 0$, and $U = (1/2s)\tanh(\pi q/s)$ for $\sigma = 1/2$. Far from the vortex row the magnetic field and the electron fluid velocity tend to zero exponentially. For $q < 1$ this configuration corresponds to an electron current sheet with thickness q surrounded by two opposite current sheets with thickness of order 1, and is similar to the configuration observed behind the laser pulse (see Fig. 1).

In our PIC simulation the velocity of the row propagation is of order $c/40$. For a pulse with $a \approx 3$ and $\omega_{pe}/\omega = 0.45$, we estimate $eB/m_e c\omega \approx 1$ which is consistent with our normalization $|\Gamma_j| = 1$. Then, from Eq. (4) we find that the distance between neighboring vortices must be approximately equal to $2c/\omega_{pe}$ in agreement with Fig. 1. From Eqs. (2) we can obtain, to the first order in perturbation amplitude, the linearized equation of motion of the vortices. Looking for solutions of the form $x_j = X\exp[\gamma t + i(j\varphi)]$, $y_j = Y\exp[\gamma t + i(j\varphi)]$, $x_k' = X'\exp[(\gamma t + ik\varphi)]$, $y_k' = Y'\exp[\gamma t + i(k\varphi)]$, for the perturbations of the coordinates of vortices from the upper and the lower chain, respectively, we find the dispersion relation which gives the relationship between the real and imaginary parts of γ and φ:

$$\gamma = \frac{i\varsigma}{\pi}\sum_{k=0}^{\infty}\frac{(k + \sigma)sq}{\rho_k'^2}K_2(\rho_k')\sin(k + \sigma)\varphi \pm \frac{1}{\pi}\left\{\left[-\sum_{j=1}^{\infty}\frac{K_1(\rho_j)}{\rho_j}(1 - \cos j\varphi) + \sum_{k=0}^{\infty}\left(\frac{K_1(\rho_k')}{\rho_k'} - \frac{q^2K_2(\rho_k')}{\rho_k'^2}\right)[1 + \varsigma\cos(k + \sigma)\varphi]\right]\left[\sum_{j=1}^{\infty}\left(\frac{K_1(\rho_j)}{\rho_j} - K_2(\rho_j)\right)(1 - \cos j\varphi) - \sum_{k=0}^{\infty}\left(\frac{K_1(\rho_k')}{\rho_k'} - \frac{(k + \sigma)^2s^2K_2(\rho_k')}{\rho_k'^2}\right)[1 - \varsigma\cos(k + \sigma)\varphi]\right]\right\}^{1/2}, \tag{5}$$

where $\varsigma \equiv \pm 1$ depends on the parity of the perturbation. The symmetrical $\sigma = 0$ vortex row is always unstable. In the limit $s \ll q \ll 1$ and $q \ll 2\pi s/\varphi \ll 1$, we recover Rayleigh's result for the growth rate $\mathcal{R}e(\gamma) = \varphi U(q\varphi)^{1/2}/s^{3/2} = \kappa U(\kappa q)^{1/2}$ of the bending instability of a finite width, fluid stream. When the perturbation

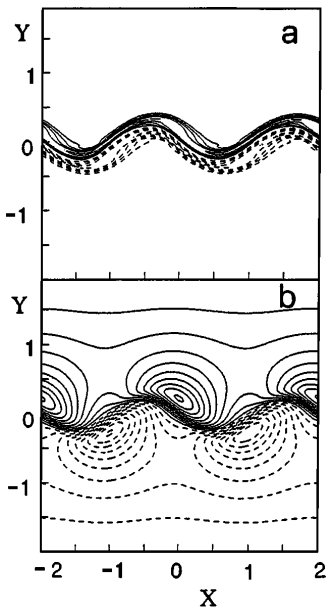

FIG. 3. Bending instability of a current sheet. (a) Curves of equal generalized vorticity Ω for $t = 19\omega_{Be}^{-1}$: $\Omega_{\min} = -1.193$, $\Omega_{\max} = 1.198$. (b) Isomagnetic curves: $B_{\min} = -0.02$, $B_{\max} = 0.02$.

wavelength is larger than 1 and q ($q < 1 < 2\pi s/\varphi$), we can estimate the instability growth rate as $\mathcal{R}e(\gamma) \approx \kappa^2 U(\kappa q)^{1/2}$. If the distance between neighboring vortices is larger than 1, $s > 1$, the growth rate is exponentially small.

In the case of the antisymmetrical vortex row with $\sigma = 1/2$ we expect a more complicated behavior of the perturbations, compared to that of the symmetrical configuration. As noted in Lamb's monograph [9], in standard hydrodynamics the antisymmetrical von Karman's vortex row is stable for $q/s \approx 0.281$. In the hydrodynamic case a point vortex is described by $(\Gamma_j/2\pi)\ln|\mathbf{r} - \mathbf{r}_j(t)|$ instead of the expression (2) which involves the Bessel function $K_0(|\mathbf{r} - \mathbf{r}_j(t)|)$. By direct inspection of Eq. (5) we see that for large distance between neighboring vortices the antisymmetric vortex row is stable when $3s^2/4 > q^2 > s/2$.

For the parameters of Fig. 1(a) the growth rate (5) leads to an e-folding time of order $30/\omega$, which is consistent with the time taken by the symmetric vortex row on the left of Fig. 1(a) to transform into an antisymmetric row with values of s and q in agreement with the above stability condition.

In order to investigate the nonlinear stage of the bending instability of a current sheet with finite width and a smooth distribution of the generalized vorticity $\Omega = B - \Delta B$, we have performed a numerical integration of Eq. (1). We have analyzed the case corresponding to a current width smaller than one (than the collisionless skin depth). The initial perturbation amplitude of 0.1 and the wavelength is equal to two.

In Fig. 3 the result of the development of the bending instability of a thin current sheet is presented. Initially, the width of the current sheet is $0.05c/\omega_{pe}$ and the total electric current inside it is one. This current sheet is formed by two generalized vorticity layers with opposite vorticity and distance $0.05c/\omega_{pe}$. In Figs. 1(a) and 3(b) we see the development of an antisymmetric vortex row. In the initial stage, for $t \leq 20\omega_{Be}^{-1}$, the instability grows exponentially in time. However, in the nonlinear stage $t \geq 20\omega_{Be}^{-1}$, the growth is not so fast.

We thank G. Bertin, J. M. Dawson, A. V. Gordeev, D. Jovanovich, V. Pavlenko, J. Rasmussen, P. V. Sasorov, P. Shukla, and V. V. Yan'kov for useful discussions. Financial Support from the Italian Ministry for Research (MURST) and from the Italian National Research Council (CNR) is gratefully acknowledged.

[1] V. I. Petviashvili and O. M. Pokhotelov, *Solitary Waves in Plasmas and in the Atmosphere* (Gordon and Breach Science Publishers, New York, 1992).
[2] R. L. Stenzel, J. M. Urrutia, and C. L. Rousculp, Phys. Rev. Lett. **74**, 702 (1995).
[3] W. Horton and A. Hasegawa, Chaos **4**, 227 (1994).
[4] S. V. Bulanov, F. Pergoraro, and A. M. Pukhov, Phys. Rev. Lett. **74**, 710 (1995).
[5] D. W. Forslund, J. M. Kindel, W. B. Mori, C. Joshi, and J. M. Dawson, Phys. Rev. Lett. **54**, 558 (1985).
[6] G. A. Askar'yan, S. V. Bulanov, F. Pegoraro, and A. M. Pukhov, JETP Lett. **60**, 241 (1994).
[7] T. Katsouleas, Phys. Rev. A **33**, 2056 (1986).
[8] R. Bingham, Nature (London) **368**, 496 (1994).
[9] A. Hasegawa and K. Mima, Phys. Fluids **21**, 87 (1978).
[10] A. V. Kingsep, K. V. Chukbar, and V. V. Yan'kov, in *Reviews of Plasma Physics*, edited by B. B. Kadomtsev (Consultant Bureau, London, 1990), Vol. 16, p. 243.
[11] G. Matsuoka and K. Nosaki, Phys. Fluids B **4**, 551 (1992).
[12] H. Lamb, *Hydrodynamics* (Cambridge University Press, Cambridge, England, 1932).
[13] G. Bertin and B. Coppi, Astrophys. J. **298**, 387 (1985).